PCCP
Physical Chemistry Chemical Physics

Accepted Manuscript

This article can be cited before page numbers have been issued, to do this please use: A. Filippov, S. BHAKTA, O. I. Gnezdilov, R. Sliz, O. N. Antzutkin and F. U. Shah, *Phys. Chem. Chem. Phys.*, 2026, DOI: 10.1039/D6CP00970K.

View Article Online
DOI: 10.1039/D6CP00970K

Fluorine-free lithium-based flexible gel electrolytes: Stretchability versus diffusivity

Andrei Filippov,[a,*] Sayantika Bhakta,[a] Oleg I. Gnezdilov,[b] Rafal Sliz,[c] Oleg N. Antzutkin,[a] and Faiz Ullah Shah[a,*]

[a] *Chemistry of Interfaces, Luleå University of Technology, SE-971 87, Luleå, Sweden*

[b] *Institute of Physics, Kazan Federal University, 420008 Kazan, Russia*

[c] *Optoelectronics and Measurement Techniques Unit, University of Oulu, Oulu FIN-90014, Finland*

* corresponding authors:

Emails: andrei.filippov@associated.ltu.se

faiz.ullah@ltu.se

Abstract

We report on the translational dynamics of ions in fluorine-free gels prepared using flexible lithium salt comprising (2-methoxyethoxy)acetate (MEA) anion, ethylene glycol (EG) and polyvinyl alcohol (PVA). ^{1}H and ^{7}Li Pulsed-Field-Gradient (PFG) NMR are performed on thin (0.2 mm) and thick (0.7 mm) films of the gels at different orientations with respect to the external magnetic field and magnetic gradients. Two diffusional decay components are observed: a slow mode linked to PVA network oscillations and a fast mode from mobile ions with diffusivities up to three orders of magnitude higher. It is found that Li^+ cations are not directly bound to the network, but they have a distribution of diffusion coefficients. A similar trend is observed for diffusivities of the organic anion, (MEA), revealed from the fast component of diffusional decays in ^{1}H PFG NMR. The diffusivities of ions have an orientational dependence on the films and are higher in thick films at the normal orientation with respect to the external magnetic field. The temperature dependence of Li^+ diffusivities does follow the Arrhenius behavior. An interesting observation is that an elongation of the gel films by stretching reduces Li^+ cation diffusivities and leads to broadening of the ^{7}Li NMR resonance lines, suggesting that transport properties of ions are strongly governed by the structural constraints and internal stresses in the gel network.

Keywords: Fluorine-free gel electrolytes, stretchability, ion diffusivity, translational dynamics, NMR diffusometry

View Article Online
DOI: 10.1039/D6CP00970K

1. Introduction

The extensive development of electronic devices for personal use as well as energy storage, conversion, and transmission require existing materials to be further developed or new materials to be created that will fulfil the growing requirements and expectations from industry and users. Liquid electrolytes, which are commonly used in various devices, are known to cause acute leakage problems in some applications, thus, devices need to be securely encapsulated [1]. Therefore, searching for a mechanically rigid solid or quasi-solid alternative for electrolytes is highly desirable.

Much progress has already been made in the development of solid and quasi-solid polymer electrolytes and their implementation in commercial devices, which have previously used liquid electrolytes to create, convert and/or transport electric energy [2,3]. Solid electrolytes increase exploitation safety, extend the scope of applicability and simplify the utility and recycling of electric energy devices. However, the use of polymers as solid matrices for liquid electrolytes has some shortcomings, particularly regarding performance at room temperature and long-term stability [4]. One of the solutions to address these drawbacks is the use of gel electrolytes [5].

Gel electrolytes are categorized into two groups: (1) Physical gels, which are formed when a liquid electrolyte is placed in a polymer matrix without the formation of chemical bonds between the polymer and solvent [6]. The physical bonds can be formed at an appropriate thermodynamic condition by a high-molecular mass polymer mixture with a liquid. (2) Chemical gels are obtained by chemical cross-linking of a polymer matrix in a liquid organic electrolyte. In both cases, gels are materials, which contain a liquid fraction but are macroscopically solid-like due to the percolating 3D network of the gelling agent. In the case of an iongel, the confined liquid phase contains an ionic liquid (IL) [7]. Dynamics of iongels have been previously studied by Quasi-elastic neutron scattering (QENS) technique [6,7,8]. QENS is very sensitive to isotopes with large incoherent neutron scattering cross section, typically samples containing many hydrogen atoms. The dynamics in the sample lead to a broadening of the spectrum of incident neutrons. QENS has been used to study dynamics of iongels, which demonstrated how confinements impact the mobility, phase transitions and ionic conductivity of the confined ionic liquids [6,8].

Iongel is a hybrid material that consists of an IL immobilized within the gel matrix. IL is an organic salt containing cations and anions that persist in liquid state at temperatures below 100

View Article Online
DOI: 10.1039/D6CP00970K

°C (by definition) [9]. Non-halogenated ILs are promising components in the development of non-volatile non-flammable halogen-free electrolytes for various electrochemical applications [10,11]. Iongels are comprised of 3D networks composed of gelator molecules, so called the gel phase, which is formed during a physical gelation phenomenon. Due to its compact cross-linking structure, iongel electrolytes may exhibit outstanding mechanical flexibility and other favorable mechanical properties of solid electrolytes.

Iongel electrolytes may also acquire desired electrochemical properties: The 3D-network may favor dissociation of a lithium salt, the principal component in electrolytes for lithium-based batteries, further resulting in a high ionic conductivity (up to 1.8×10^{-3} S/cm at ambient temperatures), a wide electrochemical window (up to 5.0 V), and a high lithium-ion transference number (0.33) [5]. Multi-nuclear diffusion NMR investigations of diffusivities of organic anions and lithium cations in gels comprised of either "hard" silica matrices of porous glasses [12] or formed by polymerization of tetraethyl orthosilicate [13], have revealed mobilities of ions comparable with those in bulk ILs.

Nuclear magnetic resonance (NMR) spectroscopy is a noninvasive method to study molecular interactions and diffusivity in multi-component and multi-phase systems, as well as opaque and porous media [10-16]. Chemical shifts and multinuclear coupling constants are used routinely for structure elucidation of ILs and the products formed by their covalent interactions with other materials. Pulsed-field-gradient (PFG) NMR (diffusion NMR) covers a wide range of time extending from milliseconds to seconds and the corresponding length of molecular displacement from sub-micrometer to micrometer. The targeted orientation of the PFG vector in NMR diffusion studies allows to explore single-axis oriented materials and two-dimensional films [17,18].

A solid-state spin-echo NMR technique can further be implemented to explore molecules and ions, which are strongly interacting with the gel matrix [19]. Le Bideau *et al.* [19] studied an IL, namely, 1-butyl-3-methylimidazolium bis-(trifluoromethanesulfon)imide, [BMIM][TFSI], confined in monolithic silica matrices by ^{1}H MAS NMR spectroscopy and temperature-dependent T_1 relaxation time measurements. They showed that the ILs' dynamics experienced only a very small slowing-down in the iongel. For measurements without spinning the ^{1}H NMR linewidth does increase with a decrease in the pore size of the silica, thus, showing that the

View Article Online
DOI: 10.1039/D6CP00970K

dynamics of confined IL is slowing down as the pore size decreases. All these ^{1}H MAS NMR experiments on monoliths, as well as on powdered iongels, give a direct evidence of the liquid-like behaviour of the confined IL with dynamics slowing down proportionally to a decrease in the pore size. A study on the relaxation times has revealed a similar behaviour for the confined IL as compared with the neat IL (above *ca*. 270 K). While at temperatures below 270 K, when the neat IL crystallizes, the confined IL still experiences a liquid-like behaviour [19].

Despite the growing interest in the internal structure, intermolecular interactions and mobility of ions in flexible gel electrolytes, this area of research is only marginally developed. In this work we employed multinuclear (^{1}H and ^{7}Li) NMR diffusion techniques to study mobility of ions in gel electrolyte films with different film thicknesses and orientations relative to the external magnetic field. The gel films are based on crosslinked polyvinyl alcohol (PVA) polymers forming 3D network matrices filled with low-melting lithium(2-methoxyethoxy)acetate (LiMEA) salt.

2. Experimental Section

2.1 Materials

(2-Methoxyethoxy) acetic acid (MEA) (ACS reagent, 99% purity; Sigma-Aldrich), lithium hydroxide monohydrate ($LiOH.H_2O$) (99.995% trace metals basis purity; Sigma-Aldrich), Polyvinyl alcohol (Polyvinylalcohol 72000, 98% purity; Merck-Schuchardt), Ethylene glycol (ReagentPlus®, ≥99% purity; Sigma-Aldrich) were used as received.

2.2 Synthesis

The gel electrolytes were prepared following the procedure described in ref. [20]. The structurally flexible ethoxy-functionalized LiMEA salt was synthesized using a neutralization method: 1 eq. lithium hydroxide monohydrate ($LiOH.H_2O$) and 1 eq. of (2-methoxyethoxy) acetic acid (MEA) were added into water and stirred for 2-4 h. After the reaction completion, the solvent was evaporated using a rotary evaporator, the LiMEA salt was obtained and dried in a vacuum oven for 2-3 days to remove residual moisture. Both purity and the chemical identity of the final product were confirmed by solution ^{1}H and ^{13}C NMR spectroscopy.

In the preparation of gel electrolytes, first, LiMEA salt was dissolved in ethylene glycol (EG) to obtain a transparent uniform solution of the concentration 0.5 or 1 M. Then, 10 mL of milliQ

View Article Online
DOI: 10.1039/D6CP00970K

water and 1 g of PVA were added to the mixture, which was further stirred at 95 °C for 4 h to obtain a homogeneous sticky solution. Then, the mixture was ultrasonicated for 5 min to remove air bubbles. Finally, the sticky mixture was poured into glass dishes and then placed in a freezer at −20 °C for 24 h, where a transparent and flexible gel membrane was formed. The gel membrane was then incubated in a vacuum-dryer (1 mbar, 293 K) for 12 hours to remove residual moisture.

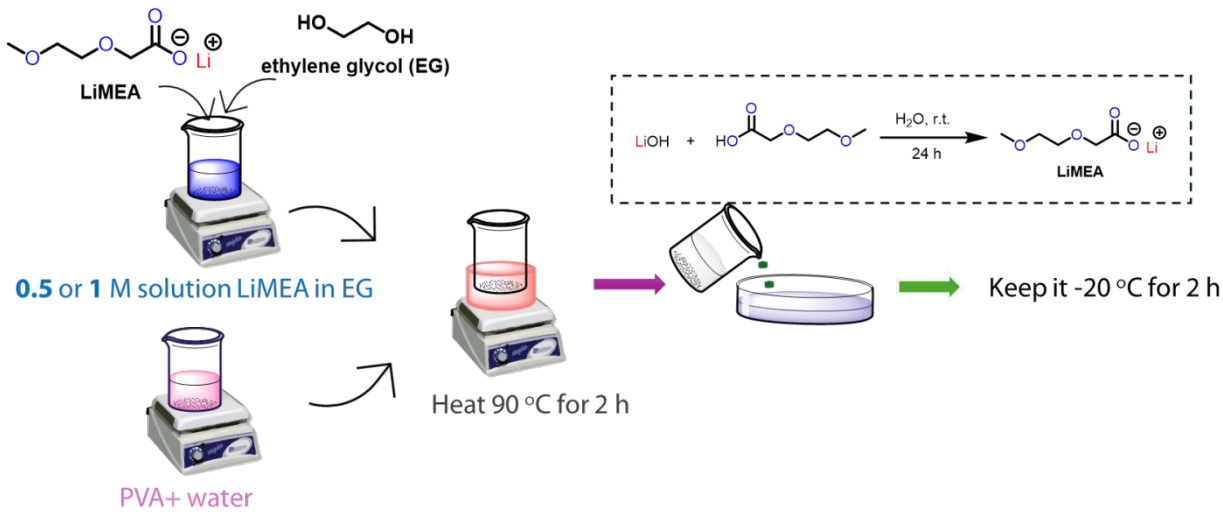

Scheme 1. Synthetic outline for preparation of the LiMEA salt and the gel electrolytes.

2.3 Preparation of samples

Two gel films with thicknesses 0.2 and 0.7 mm were prepared. The films have mechanical properties typical for elastic gels: i. e. both bending and stretching. The elongation to failure was measured to be more than 50%. The PVA network is the principal dynamic component of gels. Like a usual gel network, it consists of nodes and connections. PVA is a typical crystalline polymer: it may form gel in aqueous solutions upon a deep supercooling [21]. There is experimental evidence that the cross-links (nodes) are formed by partial crystallization of the polymer segments, in which syndiotactic sequence dominates, while sub-chains connecting the junctions (connections) consist mainly of atactic non-crystalline sequences on PVA chains. The micro-crystals at the junctions are thought to be stabilized by hydrogen bonds between the hydroxyl groups. Junctions in the PVA gel consist of syndiotactic sequences with 6-8 monomeric units [17].

The LiMEA gel was prepared as a thin film. It is initially unknown whether the gel film body is structurally and dynamically anisotropic or it pertains an isotropic structure. Thus, two types

View Article Online
DOI: 10.1039/D6CP00970K

of samples were prepared that contain the same material but differ only in the orientation of the film relative to the NMR tube axis. Since the long axis of the tube is oriented along the static magnetic field $\mathbf{B_0}$ created by the superconducting magnet of the NMR spectrometer, this allows the gel film to be oriented at either 0° or 90° relative to the "z"-direction of $\mathbf{B_0}$ and the pulsed magnetic field gradient vector **g** used in the diffusion measurements. Samples of different orientations of stacks of the gel films placed in standard 5 mm NMR tubes are schematically illustrated in Figure 1.

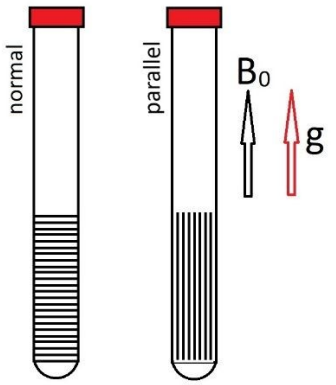

Figure 1. Schematic illustration of samples prepared for NMR measurements in standard 5 mm NMR tubes. Arrows depict directions of the static magnetic field ($\mathbf{B_0}$) and the pulsed field gradient (**g**) used for diffusion measurements.

2.4 NMR techniques

All NMR experiments were performed using Bruker Ascend Aeon WB 400 (*Bruker BioSpin AG*) NMR spectrometer. The working frequencies were 400.21 MHz for ^{1}H and 155.56 MHz for ^{7}Li. All NMR spectra were externally referenced relative to: (i) water doped with $CuCl_2$, $\delta(^1H)$ = 4.7 ppm and (ii) $LiNO_3$(aq), $\delta(^7Li)$ = -0.147 ppm. Data were processed using Bruker Topspin 3.5 software.

For diffusion measurements a Diff50 Pulsed-Field-Gradient (PFG) probe was used. The diffusional decays (DDs) were recorded using the stimulated echo (StE) pulse sequence. For a single-component diffusion, the form of the PFG DD can be described as [14] (Eq. 1):

$$A(\tau,\tau_1,g,\delta) \propto \exp\left(-\frac{2\tau}{T_2}-\frac{\tau_1}{T_1}\right)\exp\left(-\gamma^2\delta^2 g^2 D t_d\right) \quad (1)$$

View Article Online
DOI: 10.1039/D6CP00970K

Here, A is either the amplitude or the integral intensity of the NMR signal, τ and τ_1 are the time intervals in the pulse sequence; γ is the gyromagnetic ratio for the used magnetic nuclei; g and δ are the amplitude and the duration of the gradient pulse; $t_d = (\Delta - \delta/3)$ is the diffusion time; $\Delta = (\tau + \tau_1)$. D is the diffusion coefficient. In the measurements, δ was in the range of (0.5 – 3) ms, τ was in the range 1– 3 ms, and g was varied from 0.06 up to 29.73 T·m^{-1}. Diffusion time t_d was varied from 20 to 3000 ms for ^{1}H NMR experiments and from 20 to 300 ms for ^{7}Li NMR experiments. T_1 for ^{1}H and ^{7}Li varied in ranges 0.3-0.38 s and 0.45-1.2 s, respectively, increasing with temperature in the studied temperature range 293-343 K. Therefore, recycle delays during accumulation of signal transients were from 3.5 to 6 s to avoid saturation of NMR signals (longer than 5 x T_1). For statistics and validation, each experiment was repeated at least three times. Non-linear least squares regression was used to fit the experimental data with Eq. (1) to extract D values.

In the case of two molecular or ionic diffusing components differing by diffusion coefficients D_1 and D_2 with fractions p_1 and p_2, respectively, Eq. 1 transforms into the form (Eq. 2):

$$A(2\tau,\tau_1,g,\delta) = p_1 \exp\left(-\frac{2\tau}{T_{21}}-\frac{\tau_1}{T_{11}}\right)\exp\left(-\gamma^2\delta^2 g^2 D_1 t_d\right) + p_2 \exp\left(-\frac{2\tau}{T_{22}}-\frac{\tau_1}{T_{12}}\right)\exp\left(-\gamma^2\delta^2 g^2 D_2 t_d\right) \quad (2)$$

In the more general case of multi-component DDs, Eq. 1 has the following form (Eq. 3):

$$A(2\tau,\tau_1,g,\delta) = \sum_i p_i \exp\left(-\frac{2\tau}{T_{2i}}-\frac{\tau_1}{T_{1i}}\right)\exp\left(-\gamma^2\delta^2 g^2 D_i t_d\right). \quad (3)$$

From Eqs. (2) and (3) it is seen that the form of DD is affected not only by fractions p_i and diffusivities of components D_i, but also by NMR relaxation parameters of diffusing components T_{1i} and T_{2i}. This is particularly important for such multi-component systems as gels.

3. Results and Discussion

3.1 Diffusion measured on ^{1}H nuclei

^{1}H NMR spectral lines of gels represent both molecular and ionic components containing protons in their structure. However, these resonance lines are rather broad and severely overlap with each other. Therefore, we measured diffusional decays (DDs) of the integral intensities, rather than amplitudes of the ^{1}H NMR resonance lines. ^{1}H NMR DDs obtained at diffusion times from 20 ms to a few seconds, for the gel thick film (0.7 mm) oriented either normal (90°)

View Article Online
DOI: 10.1039/D6CP00970K

or parallel (0°) to the external magnetic field, $\mathbf{B_0}$, are shown in Figs. 2 and 3, respectively. For both orientations, forms of DDs are complicated and can be roughly deconvoluted in a sum of two diffusing components, which, in some particular cases, can be characterized as the "fast" and the "slow" components. The "slow" diffusion component can be readily identified on the graph.

However, the corresponding diffusion coefficient is determined with a poorer confidence, since the signal decay is ca 3-fold slower than that for the "fast" component. The apparent diffusion coefficient corresponding to the "slow" component was estimated to be in the range from $5\cdot10^{-14}$ to $5\cdot10^{-13}$ m^2/s with ca. 30% error limits. The "fast" diffusion component could not be modelled by a single exponential. Therefore, Eq. (2) does not appropriately describe the full form of the DDs. The more suitable model is either the one given by Eq. (3) or alternatively, a further modified following equation (Eq. (4)):

$$A(2\tau,\tau_1,g,\delta) = p_{fast}R_{1\,fast}(\tau_1,T_{1\,fast})R_{2\,fast}(\tau,T_{2\,fast})f_{fast}\left(\delta^2,g^2,t_d\right)+ \\ + p_{slow}\exp\left(-\frac{2\tau}{T_{2slow}}-\frac{\tau_1}{T_{1slow}}\right)\exp\left(-\gamma^2\delta^2g^2D_{slow}t_d\right) \quad (4)$$

where R_{1fast} and R_{2fast} are complex longitudinal and transverse NMR relaxation functions of the "fast" component. f_{fast} is a complex function, which describes diffusion decays of the "fast" component. To experimentally characterize averaged diffusivity corresponding to the "fast" component, an apparent average diffusion coefficient can be used:

$$D_{av} = \frac{-\partial A\left(\gamma^2\delta^2g^2t_d\right)}{\partial\left(\gamma^2\delta^2g^2t_d\right)}\Big|_{\left(\gamma^2\delta^2g^2t_d\right)\to 0} \quad (5)$$

It was found that D_{av} and D_{slow} differ by a factor of 10^3. p_{slow} is of the order 10^{-3} for the "normal" orientation (Fig. 2) and ca. 10^{-4} for the in "parallel" orientation (Fig. 3).

View Article Online
DOI: 10.1039/D6CP00970K

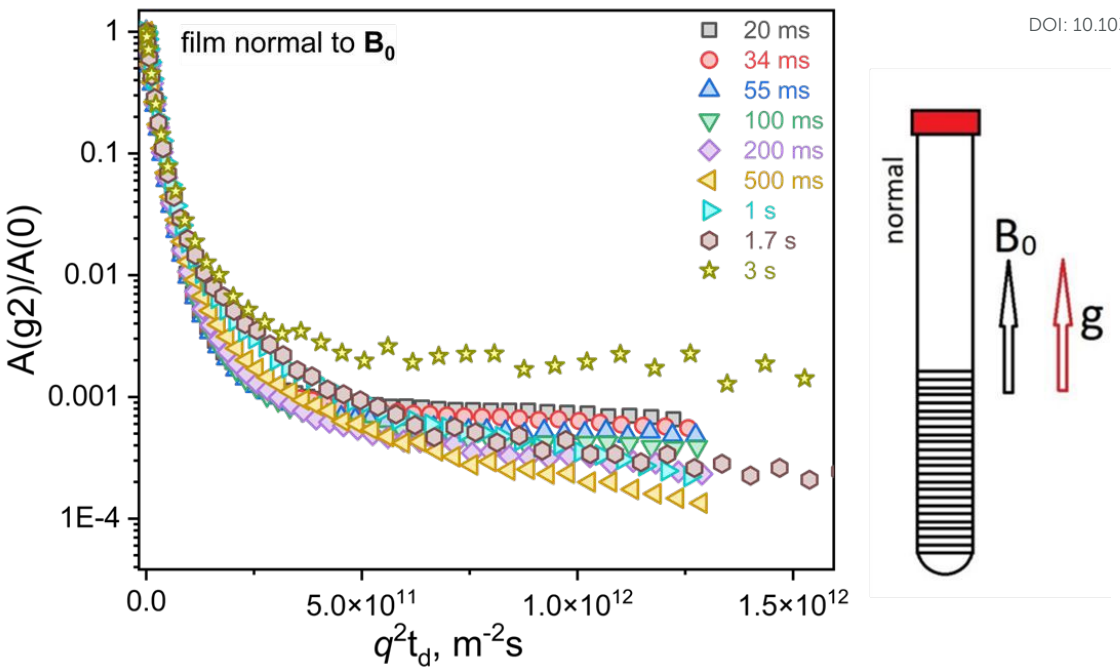

Figure 2. ^{1}H diffusion decays for a thick film (0.7 mm) of 0.5 M LiMEA gel oriented normal to $\mathbf{B_0}$ in the range of diffusion times from 20 ms to 3 s. T = 293 K.

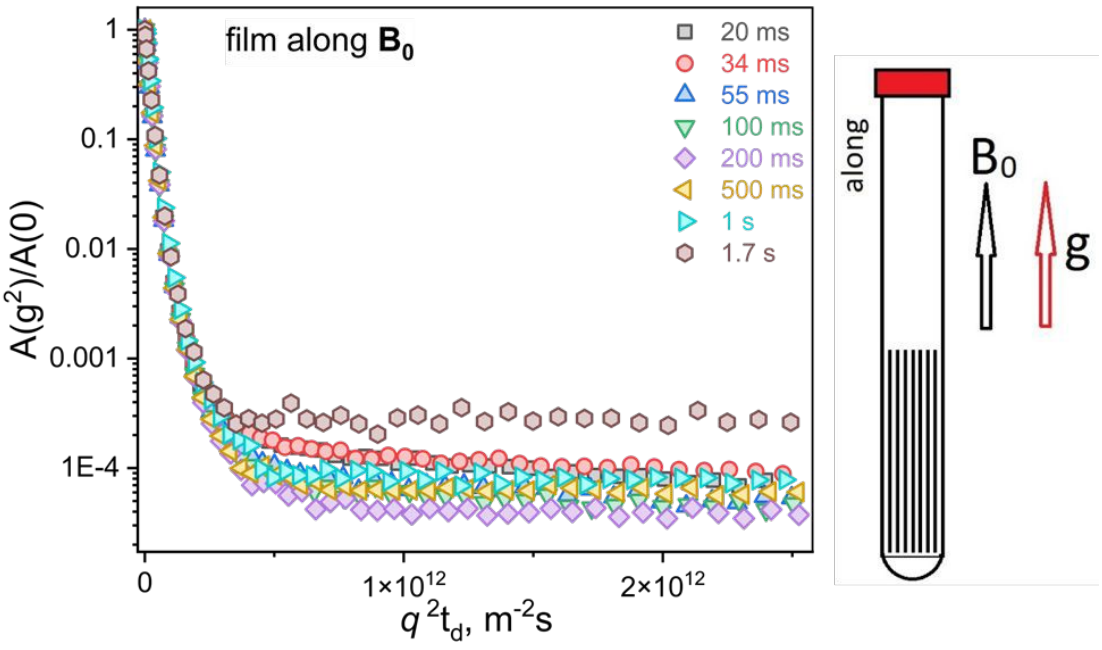

Figure 3. ^{1}H diffusion decays for a thick film (0.7 mm) of 0.5 M LiMEA gel oriented in parallel with $\mathbf{B_0}$ in the range of diffusion times from 20 ms to 1.7 s. T = 293 K.

View Article Online
DOI: 10.1039/D0CP00970K

Taking into consideration the gel-like nature of the studied gel system, we can putatively assign the "slow" component of the DDs to the gel network. Indeed, it is known that PVA may form gels [21] and the films of PVA-based gels under study are visually and mechanically consistent with this hypothesis. Further evidence comes from the analysis of the lineshapes of the ^{1}H NMR spectra corresponding to different points in the diffusion decay of the gel (Fig. 4a). First two NMR spectra (points 1 and 12 in the diffusion decay measured at the diffusion time of 20 ms, see Fig. 4a top and middle spectra) contain mainly contributions from the fast component and demonstrate resonance lines in the range from 3 to 5 ppm, which are assigned to protons of water and ethylene glycol. On the other hand, NMR spectrum obtained at point 33 in the diffusion decay (Fig. 4a, bottom) corresponds to the slow component at the experimental conditions when the fast component is already suppressed by the pulse field gradients in the diffusion experiment. Two broad resonance lines in the latter ^{1}H NMR spectrum are assigned here to protons in -OH and -CH chemical groups (near 4 ppm) and -CH_2 groups (near 1.5 - 2 ppm) of poly vinyl alcohol [22].

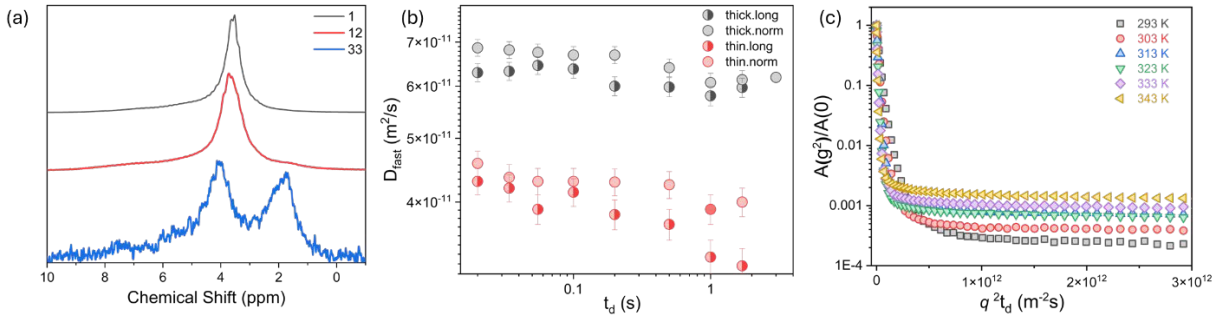

Figure 4. (**a**) Normalized ^{1}H NMR spectra of the thick film (0.7 mm) of 0.5 M LiMEA gel oriented normal to $\mathbf{B_0}$ obtained at points 1, 12 and 33 of the diffusion decay measured at the diffusion time of 20 ms in Fig. 2; (**b**) Diffusion time dependences of "fast" diffusion coefficients obtained by ^{1}H PFG NMR for 0.5 M LiMEA gel films in parallel with and normal to the external magnetic field $\mathbf{B_0}$. T = 303 K; (**c**) ^{1}H diffusion decays for a thick film (0.7 mm) of 0.5 M LiMEA gel oriented in "parallel" with $\mathbf{B_0}$ in the range of temperatures from 294 to 343 K. Diffusion time was 55 ms.

Other molecular and ionic components, which do not form the gel network and do not tightly bound to it, diffuse much faster, comparably with the system without the PVA network. This is quite typical for gels [13,23]. Diffusion of polymeric molecules is a quite complicated process, and it depends on many parameters of polymers [24]. It becomes even more complicated in the presence of the polymer chains entanglements. DDs for the thin (0.2 mm) gel film oriented

View Article Online
DOI: 10.1039/D6CP00970K

parallel with and normal to $\mathbf{B_0}$ are presented in the ESI, see Figs. S2 and S3. This diffusion NMR data also reveal both "fast" and "slow" diffusion components with different relative fractions at different diffusion times.

Diffusion coefficients corresponding to the "fast" diffusion component (D_{av}) calculated from initial slopes of the ^{1}H NMR DDs (Figs. 2 and 3, and Figs. S2 and S3 in the ESI and Eq.(5)) are shown in Fig. 4b. There is a slight trend in a decrease of diffusivities with an increase in the diffusion time. This agrees with the results obtained by Le Bideau group on gels formed with silica matrixes [6,8]: a slight confinement effect has been detected for diffusion of liquids inside pores. Diffusivities in the "thick" gel film are a factor of 1.5 - 2 higher than those in the "thin" gel film. For both "thick" and "thin" gel films, the diffusivities at the "normal" orientation of the films are up to 10% higher diffusivities at the in "parallel" orientation of the films, consistently, at all diffusion times from 20 ms to over 1 s (Fig. 4b).

Slopes of the "slow" diffusion component of DDs were modelled using the two-component deconvolution (Eq. 2) and revealed an apparent diffusion coefficient ~ 10^{-13} m^2/s, which did not show any evident dependence on the diffusion time. It was expected that for the case of a fully restricted diffusion of the network connections, the slope of D on t_d in the double logarithmic coordinates should approach (-1) [25]. This regime is, however, not evident here, probably due to a distribution of distances between nodes and even longer diffusion times required in the PFG experiments and not achievable due to relaxation.

Variation of the ^{1}H NMR DDs for the "thick" (0.7 mm) gel film oriented in "parallel" with $\mathbf{B_0}$ in the temperature range 293 K - 343 K is shown in Fig. 6. All DDs do maintain the two-component form: the "slow" and the "fast" components can be readily deconvoluted and they do have a different diffusional behavior. The slope of the "fast" component of the DDs does increase with temperature that corresponds to an increase of the diffusion coefficient from $4\cdot10^{-11}$ (at 293 K) to $1.6\cdot10^{-10}$ m^2/s (at 343 K). This temperature dependence of the diffusion coefficient in Arrhenius coordinates (lnD *vs* 1/T) is shown in Fig. S4 of the ESI. The dependence has a convex form, which formally corresponds to the VFT model [26]. The slopes of the slow decaying parts (Fig. 4c) do not change with temperature between 293 and 343 K and the diffusion coefficients are ca. 2-3 orders of magnitude smaller (D ~$1\cdot10^{-13}$ m^2/s). These

View Article Online
DOI: 10.1039/D6CP00970K

values are typical for a restricted diffusion: an increase in thermal energy does not lead to activation of the diffusion process.

From values of the diffusion coefficient ($1 \cdot 10^{-13}$ m^2/s) and diffusion time (55 ms) we can estimate a mean magnitude of oscillations of the gel network in nodes/connections as $< (2 \cdot D \cdot 0.055 \text{ s})^{0.5} \sim 0.1$ μm. These values do agree well with electrochemical strain microscopy (ESM) data obtained for similar types of PVA gel [20]. However, a relative fraction of the "slow" component (p_{slow}) does increase with temperature from ~$3 \cdot 10^{-4}$ (at 293 K) to ~$2 \cdot 10^{-3}$ (at 343K). Such an effect is usually observed in multi-component systems when diffusion components are different not only by diffusion coefficients, but also by temperature dependences of their spin-lattice (T_1) NMR relaxation times (see Eqs. (2)-(4)). Similar temperature variations for DDs were obtained for the two gel film thicknesses and for both orientations of films with respect to the external magnetic field $\mathbf{B_0}$.

3.2 Diffusion measured on ^{7}Li

^{7}Li NMR diffusion decays were measured in the range of diffusion time 20 ms – 300 ms in the signal decay of three decimal orders. It was revealed that forms of DDs are close to a single-component function (Eq. 1) for all film thicknesses and orientations of the films, except for the "normal" orientation of the "thin" (0.2 mm) gel film. Typical diffusion decays for the "thick" and "thin" films obtained at the "normal" orientation and at different diffusion times are shown in Fig. 5a and 5b, respectively. As the diffusion time increases, there is an increase in the value of the apparent diffusion coefficient of Li^+ by a factor of 1.15-1.2 (Fig. S5 in the ESI). From a thermodynamic point of view, this is an impossible situation, since the system is in the state of a thermal equilibrium.

We hypothesize here that there are small distributions of Li^+ diffusion coefficients that have only a minor effect on the observed shape of the DDs. If the slower diffusivities of the distributions are characterized with shorter T_1, an increase in the time interval τ_1 and the diffusion time t_d of the pulse sequence (Eq. 2) will lead to a decrease of contributions of components with smaller diffusivities that in turn should increase a mean apparent diffusion coefficient of lithium ions. However, an apparent single-exponential form of DDs for Li^+, caused by a small difference in diffusion coefficients, does not allow us to extract *Ds* of different diffusing components of Li^+. This situation was modelled for cases of the "normal" and the

View Article Online
DOI: 10.1039/D6CP00970K

"parallel" orientations of the thick (0.7 mm) gel film. DDs were calculated as sums of two contributions (Eq. 2) with marginal values of diffusion coefficients D_i (one obtained at the lowest and the second one at the highest diffusion times) and with apparent fractions p_i, which were supposed to vary due to differences in T_{1i} relaxation times of the two Li^+ diffusing components. Results of this modelling are presented in Figs. S6 and S7 of the ESI. It is seen that a variation in p_1 leads to a variation of DDs similarly to those obtained in the experiment, which has revealed an increase of lithium D with an increase of the diffusion time (Fig. 5a), while the form of DDs remains close to the single-component one. This affirms distribution of diffusivities of Li^+ in the gels, even in cases when DDs apparently follow a single exponential form.

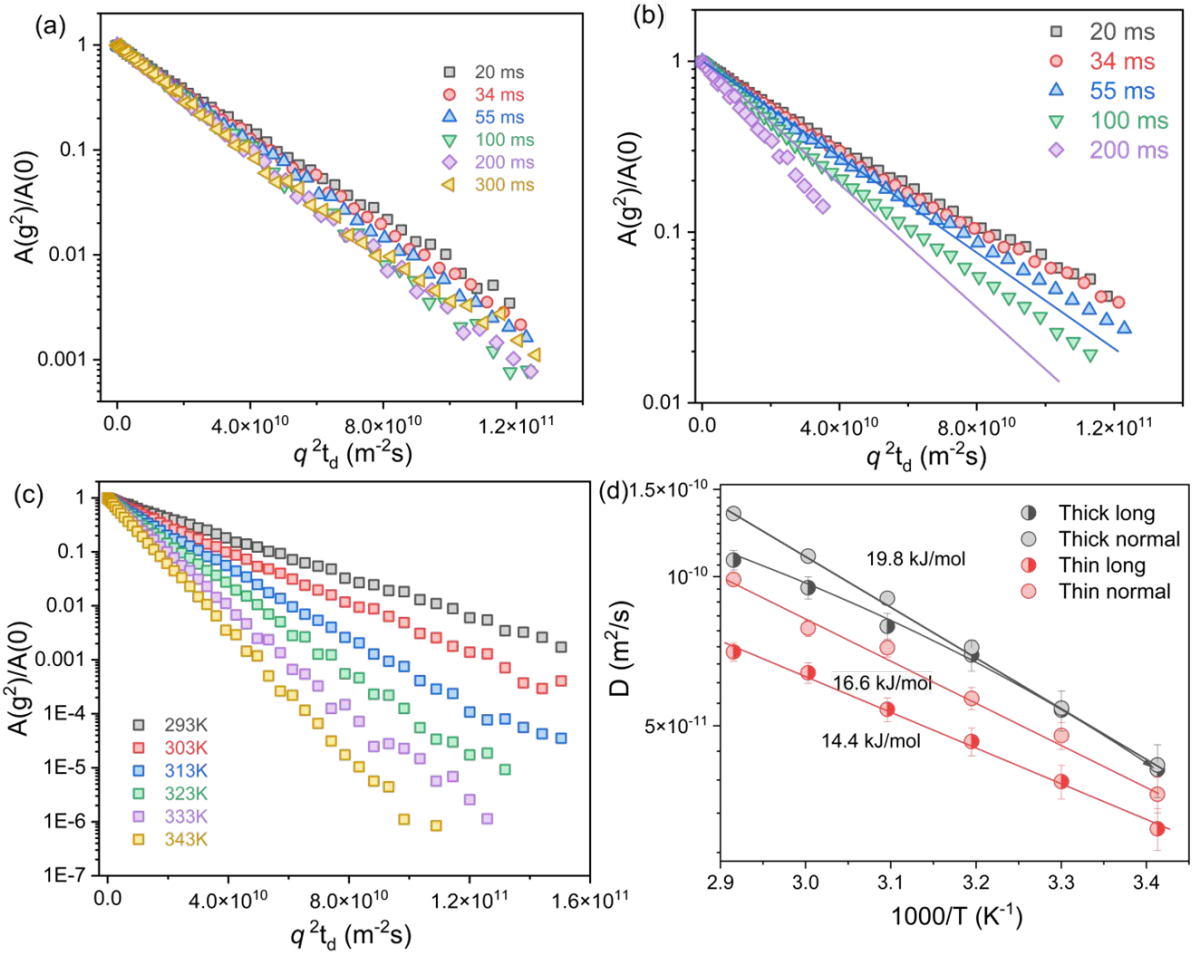

Figure 5. ^{7}Li diffusion decays for: (**a**) "thick" (0.7 mm) gel film oriented "normal" to $\mathbf{B_0}$; (**b**) "thin" (0.2 mm) gel film oriented "normal" to $\mathbf{B_0}$ at different diffusion times (denoted in the inserts). T = 293 K; (c) ^{7}Li diffusion decays for the "thick" film (0.7 mm) of 0.5 M LiMEA gel oriented "normal" to $\mathbf{B_0}$ in the range of temperatures from 293 K to 343 K. Diffusion time was 55 ms; (d) Arrhenius plot of the temperature dependence of the apparent lithium diffusion

View Article Online
DOI: 10.1039/D6CP00970K

coefficients for different gel films at different orientations with respect to the external magnetic field $\mathbf{B_0}$.

Typical temperature dependences of ^{7}Li DDs are shown in Fig. 5c. The single-component form of DDs is maintained at all temperatures. An increase in temperature leads to an increase of the slope of DDs. Similar temperature behavior for lithium DDs was observed for both "thick" and "thin" gel films and for both, in "parallel" and "normal" orientations. Temperature dependences of diffusion coefficients for all these cases are shown in Fig. 5d. It is seen that diffusivities for lithium are close to the Arrhenius form (straight lines in the Arrhenius coordinates) that is significantly different from the convex form of diffusivities obtained using ^{1}H NMR (Fig. S4 in the ESI). For the Arrhenius law for diffusion:

$$D(T) = D_0^* \cdot \exp\left(\frac{-E_D}{RT}\right) \tag{6}$$

where D_0^* is a parameter that is independent on temperature, E_D is the apparent molar activation energy of diffusion. Values of the apparent activation energies for diffusion are shown in Fig. 5d nearby the corresponding curves.

Let us analyse values of diffusion coefficients obtained by ^{1}H NMR and ^{7}Li NMR. Firstly, lithium diffusivities (D ~ 10^{-11}- 10^{-10} m^2/s, see Fig. 5d) are much higher in comparison with diffusion coefficients corresponding to the "slow" diffusion component from ^{1}H NMR DDs (~10^{-13} m^2/s), which we assigned above to the gel network. No "slow" diffusing component was detected in ^{7}Li NMR DDs with diffusion coefficients of the order of the gel network. This means that there are no Li^+ ions bound to the gel network, or if bound, these lithium species have unfavorable relaxation properties and, therefore, not detected. Comparing Ds of lithium with diffusivities of the "fast" diffusing component from ^{1}H PFG NMR (see Figs. 4b and S4 in the ESI), one could see that for the (0.7 mm) gel film diffusivities of species with protons are rather close to diffusivities of lithium. However, for the (0.2 mm) gel film, Ds of lithium are significantly lower. (Diffusivities of lithium for the thin (0.2 mm) gel film are lower than those for the thick (0.7 mm) gel film, see Fig. 5d). Also, diffusivities of lithium in the "normal" orientation are lower than those for the in "parallel" orientation. A similar trend was observed for the "fast" ^{1}H diffusion coefficients, but for lithium it is more pronounced.

View Article Online
DOI: 10.1039/D6CP00970K

3.3 Stretching of the gel films

Reversible elongation under applied mechanical force is a special property of a stretchable gel. The effect of stretching on mobility of ions in gels is of a particular interest. In the following experiment we used a ribbon of the thick (0.7 mm) gel film with a width of 3 mm and a length of 60 mm, which was tied at the ends with threads and placed in the 5 mm NMR tube, i.e. in parallel with the external magnetic field B_0 (Fig. 6). The stretching force **F** was applied along the axis of the tube, coinciding with the direction of $\mathbf{B_0}$. Elongation was increased stepwise accompanying by ^{7}Li NMR measurements at each step of controlled elongation.

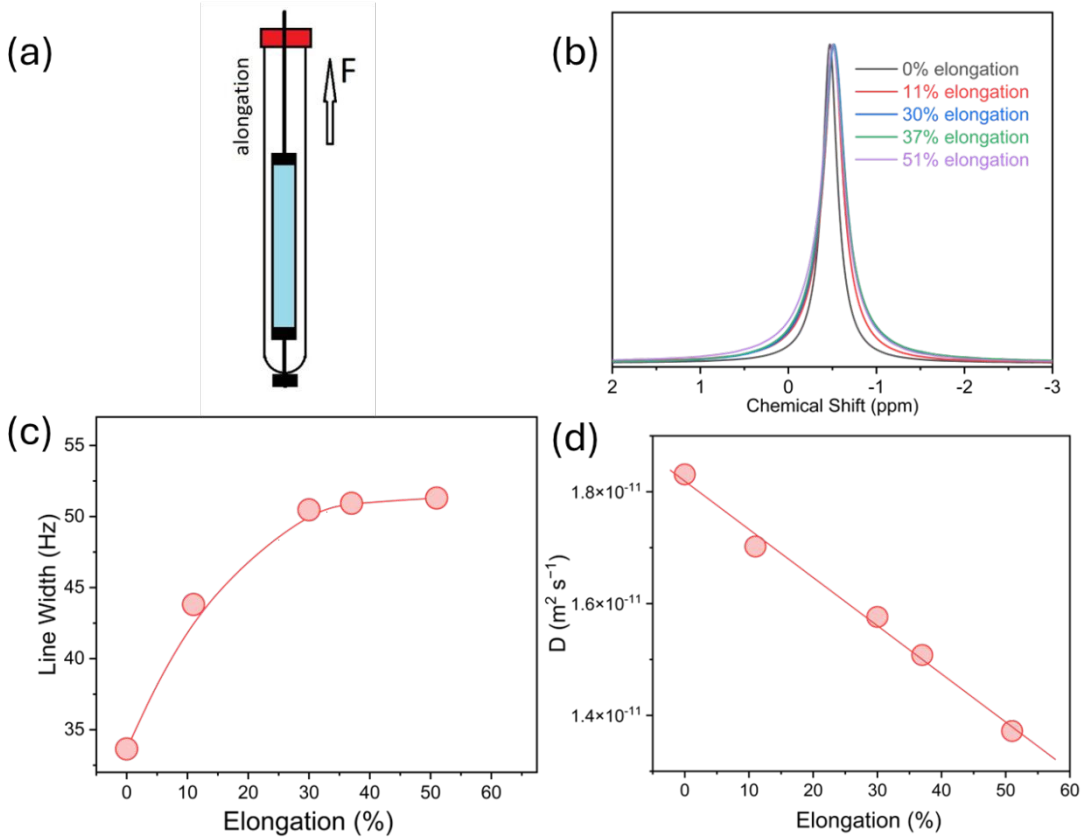

Figure 6. (**a**) Schematic presentation of the experiment with stretching of the "thick" (0.7 mm) film of 0.5 M LiMEA gel. The stretching force F is applied along the main static magnetic field ($\mathbf{B_0}$) and the pulsed field gradient (**g**), which is used for diffusion measurements; (**b**) ^{7}Li NMR spectra for the "thick" film (0.7 mm) of 0.5 M LiMEA gel oriented and stretched in parallel with the external magnetic field $\mathbf{B_0}$; (**c**) Variation of ^{7}Li NMR linewidth for the LiMEA gel film at stretching. T = 293 K; (**d**) Variation of the lithium diffusion coefficient for the "thick" film (0.7 mm) of 0.5 M LiMEA gel film upon elongation.

View Article Online
DOI: 10.1039/D6CP00970K

Fig. 6b shows ^{7}Li NMR spectra obtained at different elongations of the gel film. The chemical shift does not significantly change. The shape of the line in Fig. 6b is not purely Lorentzian, and it does not exhibit obvious biexponential behavior. Therefore, we analyzed such an average parameter of the spectra as the line width at the half height. The linewidth of the resonance line does increase as the elongation increases. The dependence of the linewidth on the elongation is shown in Fig. 6c. Initially the linewidth monotonously increases with the elongation of the film in the range 0-30% and then reaches saturation where the linewidth (ca 50 Hz) is by ca 50 % higher of its initial value (ca 34 Hz). After that the linewidth does not changes until the ribbon breaks at elongation of ca 60 %. Variation of diffusivity of lithium under the stretching process is shown in Fig. 6d. The diffusion coefficient of lithium decreases linearly by a factor of ca 1.3 in the whole range of elongation of the gel film.

Observed alterations of the lithium NMR linewidth and lithium diffusivity at the elongation is not *a priori* evident. However, it provides us with a new view on the Li^{+} interaction with the gel network. Indeed, in the used gel system the network nodes are present from the beginning of the gel preparation. We failed to prepare a gel system with the same composition and without the network nodes. On one hand, a mechanical deformation of the gel network directly demonstrates its effect on confined in the gel lithium species. The linewidth broadening (Fig. 6c) is the evidence of reducing in the intensity and an increase in an anisotropy of lithium local mobilities. On the other hand, the decrease in diffusion coefficients with an increase in the strain of the gel film (Fig. 6d) is associated with an increase in the "obstruction-to-diffusion". As it was shown, lithium is not directly bound to the gel network.

However, if the presence of gel does influence the mobility of lithium, the density of the network nodes is expected to be one of such parameters. Then elongation of the gel film in the in "parallel" direction will lead to the film shrinkage in the "normal" direction, which will increase the density of the nodes/connections of the gel network in the "parallel" direction. The latter should result in a decrease of both intensity of lithium local mobility and lithium (and "fast" diffusing proton containing species) diffusivity. Applying this idea to the dependences of lithium diffusivity on the thickness of the gel film and its orientation (Fig. 5d) it can be concluded that: 1) all films are more internally stressed in the in "parallel" direction; 2) the internal deformation of the "thin" film is higher than that of the "thick" one; 3) the broader distribution of the internal stresses is characteristic to the "normal" direction of the "thin" gel

View Article Online
DOI: 10.1039/D6CP00970K

film (Fig. 5b). Accordingly, it is seen that the internal stress does effect on the diffusivity of other non-network components of the gel (Figs. 4b and S4 in the ESI).

Intermolecular interactions in gel films include ionic interactions, van der Waals forces, hydrogen bonds and hydrophobic interactions. These forces influence the film's mechanical, electrical, and optical properties, contributing to its overall performance and functionality [7]. However, it is precisely for a rubber-like polymer (elastomer) films that the decisive role is played by interactions caused by the elastic forces of the polymer network [27]. These forces are of entropic nature. Entropy forces in elastomers arise from the tendency of polymer chains to maximize their disorder (entropy) when stretched. When an elastomer is deformed, the polymer chains are forced into a more ordered state, reducing their entropy. This reduction in entropy creates a restoring force for the return of the elastomer to its more disordered, relaxed state. PVA is a typical cross-linked elastomer. Formation of the elastomer film by external forces leads to the appearance of internal stresses. Gelation of the film leads to redistribution of elastic forces, tensions and densities in parallel with and normal to the film. Stress is defined as the internal resistance offered by a material to deformation when subjected to external loads. It is calculated as the internal force per unit area within the material [28]. Therefore, the stress is higher for thinner films.

Altogether, analyses of diffusion-time and temperature dependences of diffusivities allowed us to associate a component with the slower apparent diffusion coefficient ("slow" diffusion component) to the gel network formed by PVA. The observed (apparent) diffusion coefficients of the gel network correspond to oscillations of the gel network segments. This "networking" motion is more evident on the temperature variation of diffusion coefficients. Molecules and ions, which do not form the network (fast" diffusion component) demonstrated spectra of apparent diffusion coefficients, which we characterized with their average values. Generally, the "fast" diffusivities are up to three orders faster in comparison with the apparent diffusivities of the gel network and did not show indications of restricted diffusion due to presences of the gel network as it is seen from diffusion-time and temperature dependences of their diffusion coefficients. Diffusivities in the "thick" film are a factor of two higher, and "along" orientation gives slightly higher diffusion coefficients.

Turning to the analyses of the diffusion-time and temperature dependences of Li^+ diffusion decays, which showed that Li^+ is not directly bound to the gel network. There are distributions

View Article Online
DOI: 10.1039/D6CP00970K

of Li^+ diffusion coefficients for both gel thicknesses and both orientations. This agrees well with the previously observed separation of Li^+ ions in the presence of host matrix [6]. Mean values of Li^+ diffusion coefficients are close to the no-network molecules and ions of the system. The Li^+ diffusivities follow the same trend as the "fast" diffusivities measured by ^1H NMR: Li^+ diffusivities for the "thick" gel film are higher than those of "thin" ones, and diffusivities in the "normal" direction are distinctly higher than those of "along". On the other hand, temperature dependences followed the Arrhenius dependence, but not to VFT model observed for the "fast" ^1H diffusivities.

4. Conclusions

The PFG NMR studies of the flexible lithium-based gel electrolytes revealed two distinct dynamic components: a slow diffusion mode arising from the oscillatory motions of the PVA network and a fast mode associated with the non-networked molecules and ions, with diffusivities differing by up to three orders of magnitude. Film thickness, orientation, and mechanical elongation significantly influence ionic/molecular diffusivities, as the thicker films at normal orientation showed higher values, while the elongation decreased the Li^+ mobility. Li^+ ions are found to be not directly bound to the network and exhibit Arrhenius-type temperature dependence, in contrast to the VFT behavior of the fast ^1H diffusivities. These results demonstrate that ion transport in gels is strongly governed by the structural constraints and internal stresses of the polymer network.

Acknowledgements

The financial support from the European Regional Development Fund (Interreg Aurora, project number: 20366551) is gratefully acknowledged. We are grateful to the Foundation in memory of J.C. and Seth M. Kempe and the LTU laboratory fund, which provided grants that funded the purchase of the NMR equipment. Diffusion measurements were partly carried out using funds from a subsidy allocated to Kazan Federal University for the implementation of the state assignment in the field of scientific activity FZSM-2026-0030.

Conflict of Interest

The authors declare no conflict of interest.

View Article Online
DOI: 10.1039/D6CP00970K

References

1. Z. Moradi, A. Lanjan, R. Tyagi, S. Srinivasan, Review on current state, challenges, and potential solutions in solid-state batteries research, *J. Energy Storage*, 2023, **73**, 109048.

2. L. Long, S. Wang, M. Xiao and Y. Meng, Polymer electrolytes for lithium polymer batteries, *J. Mater. Chem. A*, 2016, **4**, 10038-10069.

3. J. Mu, S. Liao, L. Shi, B. Su, F. Xu, Z. Guo, H. Li and F. Wei, Solid-state polymer electrolytes in lithium batteries: latest progress and perspective, *Polym. Chem.*, 2024, **15**, 473-499.

4. N.G. Ningappa, A.K. Madikere Raghunatha Reddy, K. Zaghib, Advanced polymer electrolytes in solid-state batteries, *Batteries*, 2024, **10**, 454.

5. L, Liang, X. Chen, W. Yuan, H. Chen, H. Liao, Y, Zhang, Highly conductive, flexible, and nonflammable double-network poly(ionic liquid)-based ionogel electrolyte for flexible lithium-ion batteries, *ACS Appl. Mater. Interfaces*, 2021, **13**, 25410–25420.

6. C. V. Cerclier, J.-M. Zanotti, J. Le Bideau, Ionogel based on biopolymer–silica interpenetrated networks: dynamics of confined ionic liquid with lithium salt, *Phys. Chem. Chem. Phys.*, 2015, **17**, 29707-29713.

7. X. Fan, S. Liu, Z. Jia, J. J. Koh, J. C. C. Yeo, C.-G. Wang, N. E. Surat'man, X. J. Loh, J. Le Bideau, C. He, Z. Li and T.-P. Loh, Ionogels: recent advances in design, material properties and emerging biomedical applications, *Chem. Soc. Rev.*, 2023, **52**, 2497-2527.

8. S. Mitra, C. Cerclier, Q. Berrod, F. Ferdeghini, R. De Oliveira-Silva, P. Judeinstein, J. Le Bideau, J.-M. Zanotti, Ionic liquids confined in silica ionogels: Structural, thermal, and dynamical behaviors, *Entropy*, 2017, **19**, 140.

9. Z. Lei, B. Chen, Y.-M. Koo, D. R. MacFarlane, Introduction: Ionic Liquids, *Chem. Rev.*, 2017, **117**, 10, 6633–6635.

10. M. Ahmed, A. Kushwaha, A Filippov, P Johansson, F. U. Shah, Saccharinate-based ionic liquids and lithium battery electrolytes, *Batteries & Supercaps*, 2025, e202400758.

11. M. Ahmed, A. Filippov, P. Johansson, F. U. Shah, Pyrrolidium- and imidazolium-based ionic liquids and electrolytes with flexible oligoether anions, *ChemPhysChem*, 2024, **25**, e202300810.

12. A. Filippov, M. Rudakova, V.P. Archipov, F. U. Shah, Nanoconfinement effects on the dynamics of ionic liquid-based electrolyte probed by multinuclear NMR, *Soft Matter*, 2024, **20**, 8436 – 8445.

View Article Online
DOI: 10.1039/D6CP00970K

13. A. Filippov, M. Karlsson-Broström, R. Gimatdinov, F. U. Shah, O.N. Antzutkin, Ion dynamics in an iongel electrolyte based on fluorine-free ionic liquid probed by multinuclear NMR, *Phys. Chem. Chem. Phys.*, 2025, **27**, 8221 - 8229.

14. P. T. Callaghan, Principles of Nuclear Magnetic Resonance Microscopy. **1991**. Clarendon, Oxford.

15. C. Iacob, J. R. Sangoro, W. K. Kipnusu, R. Valiullin, J. Kärger and F. Kremer, Charge transport and diffusion of ionic liquids in nanoporous silica membranes, *Soft Matter*, 2012, **8**, 289-293.

16. A. Filippov, O. N. Antzutkin, V. P. Arkhipov, O. I. Gnezdilov, Diffusivity of ethylammonium nitrate protic ionic liquid confined in porous glasses, *J. Mol. Liq.*, 2022, **356**, 118998.

17. A. Filippov, G. Orädd, G. Lindblom, The effect of cholesterol on the lateral diffusion of phospholipids in oriented bilayers, *Biophys. J.*, 84, 3079-3086.

18. A. Filippov, O. I. Gnezdilov, N. Hjalmarsson, O. N. Antzutkin, S Glavatskih, I. Furo, M. W. Rutland, Acceleration of diffusion in ethylammonium nitrate ionic liquid confined between parallel glass plates, *Phys. Chem. Chem. Phys.*, 2003, **19**, 25853-25858.

19. J. Le Bideau, P. Gaveau, S. Bellayer, M.-A. Neouze, A. Vioux, Effect of confinement on ionic liquids dynamics in monolithic silica ionogels: ^{1}H NMR study, *Phys. Chem. Chem. Phys.*, 2007, **9**, 5419–5422.

20. J. Liu, Z. Khanam, S. Ahmed, T. Wang, H. Wang, S. Song, Flexible antifreeze Zn-ion hybrid supercapacitor based on gel electrolyte with graphene electrodes, *ACS Appl. Mater. Interfaces*, 2021, **13**, 16454−16468.

21. F. Tanaka, K. Nishinari, Junction multiplicity in thermoreversible gelation, *Macromolecules*, 1996, **29**, 3625-3628.

22. I. Korbag, S.M. Saleh, Studies on the formation of intermolecular interactions and structural characterization of polyvinyl alcohol/lignin film, *Int. J. Environ. Stud.*, 2016, **73**, 226-235.

23. I. R. Gafurov, V. D. Skirda, A. I. Maklakov, S. P. Perevezentseva, Y. A. Zimkin, NMR study of the structure of aqueous gelatine gels and the process of their formation, *Polymer Science USSR*, 1989, **31**, 292-300.

24. E. J. Bailey, K. I. Winey, Dynamics of polymer segments, polymer chains, and nanoparticles in polymer nanocomposite melts: A review, *Progr. Polym. Sci.*, 2020, **105**, 101242.

25. V. Skirda, A. Filippov, A. Sagidullin, A. Mutina, R. Archipov and G. Pimenov, in: Fluid Transport in Nanoporous Materials. Book series: *NATO Science Series II-Mathematics Physics and Chemistry*. 2006, **219**, 255-278.

26. G. S. Fulcher, Analysis of Recent Measurements of the Viscosity of Glasses, *J. Am. Ceram. Soc.*, 1992, **75**, 1043–1055.

27. L.R.G. Treloar (1975), Physics of Rubber Elasticity, Oxford University Press, ISBN 9780198570271.

28. Materials Science of Thin Films (Second Edition). Deposition and Structure. Chapter 12 - Mechanical Properties of Thin Films. 2002, Pages 711-781.

View Article Online
DOI: 10.1039/D6CP00970K

Data availability statement

The data supporting this article have been included as part of the Supplementary Information.